Nonstandard Farey Sequences in a Realistic Diode Map

1991 Europhys. Lett. 16 635

(http://iopscience.iop.org/0295-5075/16/7/005)

EUROPHYSICS LETTERS 14 October 1991

Europhys. Lett., **16** (7), pp. 635-641 (1991)

Nonstandard Farey Sequences in a Realistic Diode Map.

G. PEREZ, SUDESHNA SINHA and H. A. CERDEIRA (*)

International Centre for Theoretical Physics - P.O.B. 586, 34100 Trieste, Italy

(received 13 June 1991; accepted in final form 29 August 1991)

PACS. 05.45 – Theory and models of chaotic systems.

Abstract. – We study a realistic coupled-map system, modelling a *p-i-n* diode structure. As we vary the parameter corresponding to the (scaled) external potential in the model the dynamics goes through an exchange of stability bifurcation and a Hopf bifurcation. When the parameter is increased further, we find evidence of a sequence of mode-locked windows embedded in the quasi-periodic motion. These periodic attractors can be ordered according to a Farey tree that is generated between two parent fractions 2/7 and 2/8, where 2/8 implies *two distinct coexisting* attractors with $\rho = 1/4$, and the correct structure is obtained only when we use the parent fraction 2/8. So, unlike a regular Farey tree, here numerator and denominator of the Farey fractions need not be relative primes. We also checked that the positions and widths of these windows exhibit well-defined power law scaling. When the potential is increased further, the Farey windows still provide a «skeleton» for the dynamics, and within each window there is a host of other interesting dynamical features, including multiple forward and reverse Feigenbaum trees.

Coupled maps (CM), as models of many-component nonlinear physical, chemical and biological systems, have been the focus of much research interest. For instance, realistic models of convection in conducting fluids, a.c.-driven d.c. SQUIDS, instabilities in solids, neurodynamics and polyatomic molecules interacting with strong IR radiation fields such as CO_2 lasers, involve coupled oscillatory processes [1]. Extensive studies have mostly been devoted to systems of coupled logistic maps. Here we study a very different kind of CM, and elucidate the features of its dynamics.

We consider here a CM which describes an interesting physical problem [2], namely a device with a *p-i-n* diode structure, consisting of two oppositely doped silicon regions separated by a layer of intrinsic silicon. When the *p-i-n* diode is reverse biased the two regions of fixed charges are separated by the relatively long intrinsic Si region, which acts as an insulator. The device under consideration is kept at low temperature, with a reverse bias voltage $V_0 + V(t)$, where $V(t)$ is in synchronism with the mechanism that produces the change in the density of carriers. The peaks of $V(t)$ make the field at both junctions slightly above the «critical value» for an avalanche process to develop. So a slight change in the density of carriers will trigger an avalanche. During the lower half-cycle of $V(t)$ the field is subcritical, stopping the avalanche and sweeping away the electron and hole charge clouds.

(*) Also at Universidade Estadual de Campinas, Instituto de Física, 13801 Campinas, SP Brazil; Associate Member of the INFN (Istituto Nazionale di Fisica Nucleare).

Such a device will produce a current with an oscillating component in the following way: a carrier crossing, say, the left junction will produce two charge clouds, one of which moves to the right. As it reaches the second junction it will produce two charge clouds, one of them moving towards the left, and so on. This will produce an oscillation in the current, whose frequency will depend on the distance between the junctions, and should be much higher than the frequency of the bias voltage.

We consider here a simplified one-dimensional structure, with two slabs (representing the junctions), with an electric field applied to them, strong enough to produce an avalanche, separated by a region where the field is weak enough so that particles just drift with a constant velocity (the intrinsic region). Since the behaviour of the density of carriers at a certain slab end depends linearly on the density of carriers of opposite sign at the slab end where it bounced before, we may represent these successive densities as the coupled map [2]:

$$\begin{cases} x_{n+1} = c y_n \exp\left[\dfrac{-1}{|V - x_n|}\right], \\ y_{n+1} = c x_{n+1} \exp\left[\dfrac{-1}{|V - y_n|}\right], \end{cases} \tag{1}$$

where x and y are the (scaled) densities of the negative and positive carriers, respectively, V is the (scaled) potential applied across the junction and c is a parameter associated with the characteristics of the sample whose particular dependence is not of interest here. The discrete time variable n represents successive «bounces» of clouds of charge. The important physical feature of this system, very different from the usual well-known unimodal maps, is the *exponential* in eq. (1), which is typical of the density of a cloud of charge leaving a junction where a voltage is applied.

We investigate the features of the dynamics as a function of the (scaled) voltage V, as clearly it is the parameter we can control externally. Figure 1 shows the bifurcation diagram for V and it is evident that the variation of this parameter gives rise to a very rich and interesting reportoire of phenomena. The dynamics starts with a fixed-point behaviour. The fixed points of the map are $x^{(1)} = y^{(1)} = 0.0$ and $x^{(2)} = y^{(2)} = V - 1/\log c$. The Jacobian is given by

$$J = \begin{vmatrix} \dfrac{x_{n+1}\,\mathrm{sign}\,(x_n - V)}{(V - x_n)^2} & \dfrac{x_{n+1}}{y_n} \\ \dfrac{y_{n+1}\,\mathrm{sign}\,(x_n - V)}{(V - x_n)^2} & \dfrac{y_{n+1}}{y_n} + \dfrac{y_{n+1}\,\mathrm{sign}\,(y_n - V)}{(V - x_n)^2} \end{vmatrix}. \tag{2}$$

At a fixed point J becomes

$$J = \begin{vmatrix} q & 1 \\ q & 1+q \end{vmatrix}, \tag{3}$$

where $q = x^{(i)}/(V - x^{(i)})^2$, $i = 1, 2$. For the first fixed point $(x^{(1)}, y^{(1)})$, the absolute values of the eigenvalues of J are 0 and 1, and so the stability of this fixed point is always marginal ([1]). The

([1]) Note that these marginally stable points, $x^{(1)} = y^{(1)} = 0$, sometimes appear in the simulations (see fig. 1 and 5).

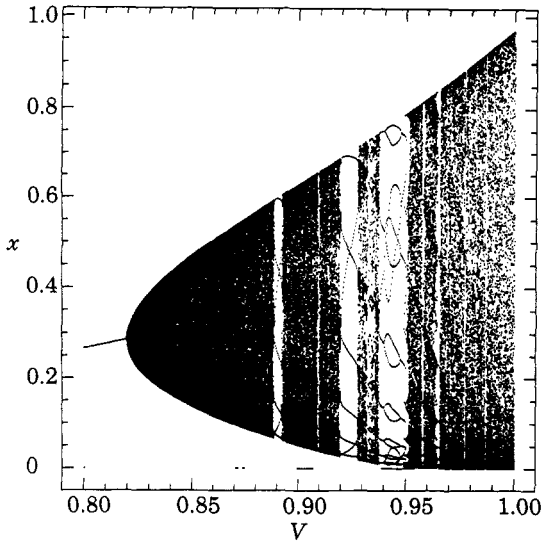

Fig. 1.

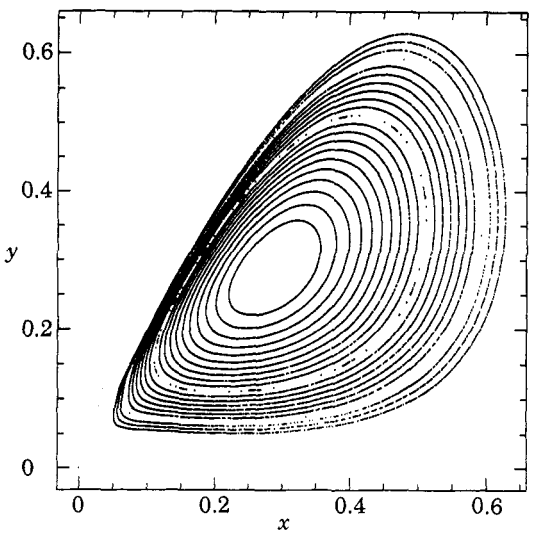

Fig. 2.

Fig. 1. – Bifurcation diagram as a function of voltage V, at $c = 6.5$. 100 random initial conditions, chosen from the range $x \in [0.05 \div 0.75]$ and $y \in [0.1 \div 0.8]$, are plotted here.

Fig. 2. – Stable attractors in phase space ((x, y)-plane) for different values of V, after the Hopf bifurcation ($c = 6.5$).

eigenvalues for the second fixed point are

$$\lambda = \log c\,[1 - V \log c] + 1/2 \pm \sqrt{\log c\,[1 - V \log c] + 1/4}\,,$$

and at V just greater than $1/\log c$ their absolute values become smaller than 1, and there is an exchange of stability bifurcation ([2]). So the second fixed point becomes stable. This fixed point retains stability until the absolute value of one of the λ's exceed 1, where the system undergoes a Hopf bifurcation, giving rise to radial attractors. In this work, we set the value of $c = 6.5$. For this value of c the two bifurcations occur at $V_{\text{e.o.s.}} = 0.534\,244$ and $V_{\text{Hopf}} = 0.819\,661$.

The stable phase space attractors associated with various values of V after the Hopf bifurcation are one-dimensional closed curves (see fig. 2), with the unstable fixed point $x^{(2)} = y^{(2)} = V - 1/\log c$ in its interior. This diode map then effectively behaves as a circle map [4], and can be well described by an angle variable $\Theta = \text{tg}^{-1}(y = y^{(2)})/(x - x^{(2)})$. So this system can be considered as a *nonstandard example of a circle map arising from a realistic model of a device.*

There is no *a priori* reason to expect this map to be reducible to the standard circle map, $\theta' = \theta + \Omega + K \sin\theta$. So, it becomes of importance to find, through numerical experiments, the phenomenology of this map with respect to changing V, in order to be able to make contact with experiments. In particular, we would also like to check phenomenologically the

([2]) This is, however, a slightly uncommon exchange of stability bifurcation, since only one branch of the fixed-point solutions changes stability, and the other branch remains marginally stable both before and after the bifurcation. See, for instance, [3].

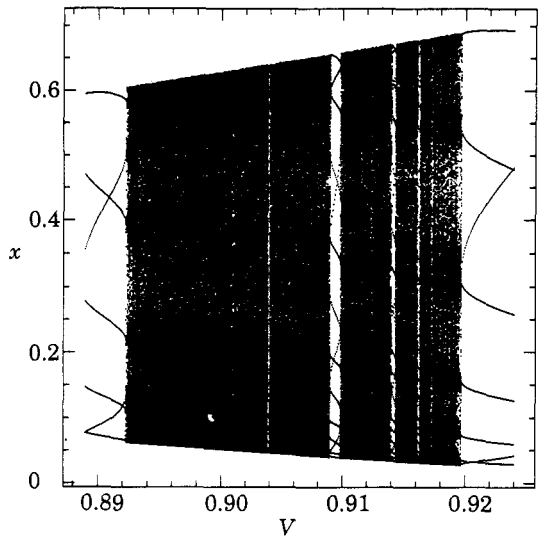

Fig. 3.

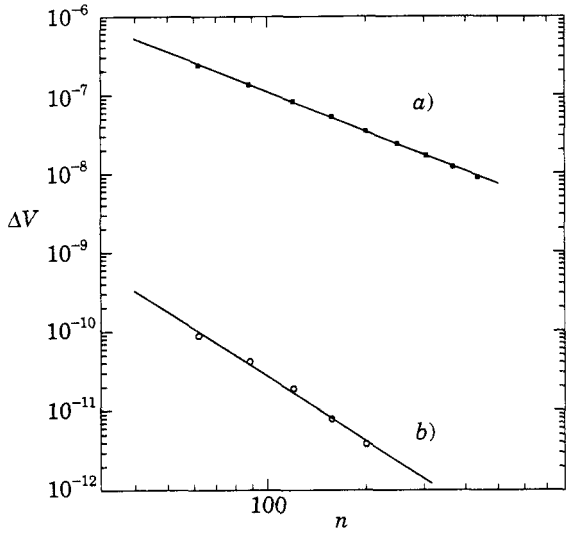

Fig. 4.

Fig. 3. – Bifurcation diagram of the region of parameter space between the two basic 2/7 and 2/8 windows, showing the series of narrower windows whose winding numbers are related to the nonstandard Farey sequence.

Fig. 4. – Plot of ΔV *vs.* n for the family with $R = (2n)/(7 + 8(n-1))$ (this family consists of windows with $Q = 7 + 8 \times 1 = 15$, $7 + 8 \times 2 = 23$, and so on) for *a*) $\Delta V \equiv d_n$, the distance of the n-th window from the 8 window. *b*) $\Delta V \equiv w_n$, width of the n-th window.

presence of mode locking, what Farey sequences we encounter (if any), and whether scaling holds as we cut across the Arnold tongues in a complicated curve [5].

We find that in the segment of parameter space, $V \sim 0.89 \div 0.92$, there are several periodic windows, supporting attractors with Farey tree properties [5]. The first such rather wide window supports an attractor with winding number $\rho = 2/7$. Between the Hopf bifurcation and this 7 window, only quasi-periodic motion is evident, characterized by limit cycles (continuous 1-dimensional curves in phase space) whose largest Lyapunov exponents are zero. After the 7 window there is another wide window with 8 lines. The interesting thing about this 8 window is that it is actually comprised of *two distinct coexisting attractors*, each with periodicity 4 and $\rho = 1/4$. In the Θ-V space the two attractors making up the 8 window appear intercalated. Between these 7 and 8 windows we find a series of narrower windows whose winding numbers can be obtained from Farey tree generated between the fractions $R = 2/7$ and $R = 2/8$, where the width of the window depends on its position in the Faree tree [5]. The significant feature to note here is this: the correct sequence of Farey fractions is *not* generated by the parent fraction 1/4, but we must use 2/8 as the parent in generating the tree. So the coexistence of attractors must be taken into account in the process of constructing the Farey sequence. This brings us to an important distinction between this Farey tree and a regular Farey tree. *Here the numerator P and denominator Q of the Farey fraction need not be relatively prime, and* $R \equiv P/Q = (2 \times p)/(2 \times q)$ *is permissible.* Whenever we have such a fraction, the window actually supports two coexisting attractors, each with $\rho = p/q$. Otherwise, if P and Q are relative prime, ρ is equal to R.

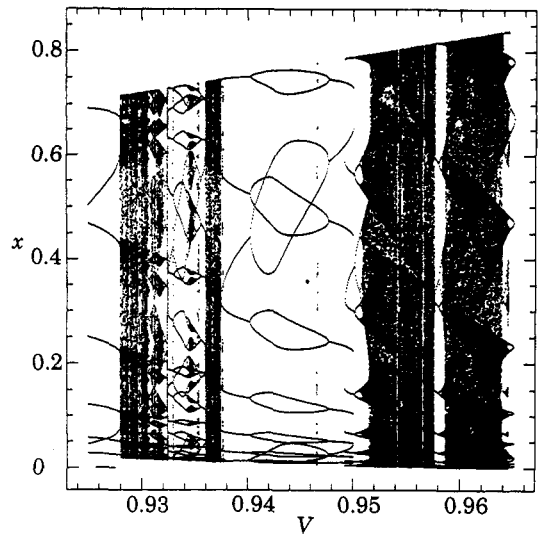

Fig. 5. – Bifurcation diagram of the region of parameter space beyond the 2/8 window, showing the 2/9 window with pitchfork and period doubling bifurcations.

Figure 3 shows a series of these windows. The 4/15 window between the basic 2/7 and 2/8 windows is easily seen, and on closer examination we can find the 6/23 window between the 4/15 and 2/8 windows, and the 6/22 window (which implies two attractors with $\rho = 3/11$) between the 4/15 and 2/7 windows, and so on. We have located a large amount of windows over several generations.

The relevant Farey tree is exhibited in the following table, for the first 3 generations:

2/7														2/8
							4/15							
			6/22								6/23			
		8/29				10/37				10/38				8/31

It is useful to consider subsets of these windows as «families», whose members are generated by a running index. For instance, the set of windows with $R = (2n)/(7 + 8(n - 1))$ can be considered to be a family with running index n. This family will then have as members windows with number of lines $Q = 7, 15, 23, 31, \ldots$. The family will accumulate as $n \to \infty$ at the 8 window.

We expect the positions of windows of a certain family, accumulating, say, at the 8 window, to obey a scaling form

$$d_n = d_0 n^{-\alpha}, \tag{4}$$

where the running index is n, and d_0 is a proportionality constant whose value depends on the particular family considered, and d_n is the distance from the n-th window of the family ([3])

([3]) Here we measure the distance from the centre of the window. The scaling properties however are not crucially dependent on the manner in which d_n is measured, and distances measured from the edge of the windows give quite the same result.

to the parent window where this series accumulates. Note here that different families accumulating at a certain window are intercalated in a regular fashion. For instance, windows with number of lines $Q = 14 + 8(2n + 1)$ always occur between windows with $Q = 7 + 8n$ and $Q = 7 + 8(n + 1)$, where $n = 0, 1, 2, \ldots$. If the different families accumulating at a certain window scaled differently, then there would be mismatches in the intercalation. Since such mismatches are not seen to occur, we expect α to be independent of the families, as has indeed been observed.

The scaling was verified through numerical experiments over several generations. For numerical convenience, we have concentrated on families accumulating at the 8 window. Figure 4 shows d_n *vs.* n for the family, with $R = (2n)/(7 + 8(n - 1))$. It is clear that scaling holds very well, and the exponent α is equal to 1.68 ± 0.01. We also checked that the widths of the windows scaled with the number of lines in the window, as a power law, given by

$$w_n = w_0 n^{-\gamma}, \tag{5}$$

where w_0 is a constant whose value depends on the particular family considered, and w_n is the width of the n-th window of the family. Figure 4 shows this power law dependence of the widths of the windows, for the family with $R = (2n)/(7 + 8(n - 1))$. We find that the value of γ is 2.70 ± 0.01, that is $\gamma \approx \alpha + 1$. It is clear that we can also interpret the Farey tree as families accumulating at the 7 window, for instance those with $R = (2n)/(8 + 7(n - 1))$. These families should also display scaling, with possibly different exponents. The widths of the windows in these families scale down very fast, which make them very difficult to locate as they are extremely narrow.

The complicated dynamics following this region has one wide window which supports an attractor with $R = 2/9$. Now the 9 window has the additional complexity that each of the 9 branches of the attractor undergoes pitchfork (but not period doubling) bifurcations and we have a region of coexisting 9 attractors. These later disappear, and just before that another set of 9 lines appears which undergo a Feigenbaum period doubling cascade, leading to chaos. Further, between the 2/8 and 2/9 windows, a 4/17 window can be seen, and between the 4/17 and 2/8 windows, a 6/25 window. Of course, in these regions of parameter space, the windows provide only a «skeleton» for the system, and there are many very complicated dynamical features, within the windows themselves (see fig. 5). Most of these additional features (if not all) are Feigenbaum trees, manifested as numerous forward and reverse period doubling bifurcations. This behaviour is analogous to the one observed in the standard circle map, for large values of its nonlinear coupling K.

In summary, we have studied the dynamics of a coupled-map system describing a realistic *p-i-n* device, with respect to changing the external potential, which is the relevant parameter from the experimental point of view. The system undergoes an exchange-of-stability bifurcation and then a Hopf bifurcation, after which it behaves effectively as a circle map, displaying a Farey sequence of attractors characterized by clearly evident power law scaling properties. The remarkable thing about this Farey sequence is that it is generated between two periodic windows with Farey fractions $R = 2/7$ and $R = 2/8$, where the 2/8 arises from *two distinct coexisting attractors with winding numbers equal to* 1/4. So $R = (2 \times p)/(2 \times q)$ is permissible, and whenever we have such a Farey fraction the window supports two coexisting attractors, each with $\rho = p/q$. As the potential is increased further, the Farey windows still provide the «skeleton» of the dynamics, but within the windows numerous forward and reverse bifurcations can be seen. This system, then, is a nonstandard example of a circle map, arising in a nonobvious way from a realistic physical model which has the scope of being checked out experimentally.

* * *

We are grateful to the Condensed Matter Group at the International Centre for Theoretical Physics for their hospitality.

REFERENCES

[1] HOGG T. A. and HUBERMAN B. A., *Phys. Rev. A*, **29** (1984) 275; LIBCHABER A. and FAUVE S., in *Melting, Localization and Chaos*, edited by R. K. KALIA and P. VASHISHTA (North Holland, New York, N.Y.) 1982; KANEKO K., *Phys. Rev. Lett.*, **65** (1990) 1391; FERRETTI A. and RAHMAN N. K., *Chem. Phys. Lett.*, **140** (1987) 71; GLASS L. and MACKEY M. C., *From Clock to Chaos* (Princeton University Press, Princeton, N.J.) 1988; *Chaos*, edited by A. V. HOLDEN (Manchester University Press, Manchester) 1986; FREEMAN W., *Brain Res. Rev.*, **11** (1986) 259; KITTEL A., CLAUSS W., RAN U., PARISI J., PEINKE J. and HUEBNER R. P., *XX International Conference in Semiconductors, Greece, 1990.*

[2] CERDEIRA H. A., COLAVITA A. A. and EGGARTER T. P., to appear in *Applied Chaos*, edited by J. H. KIM and J. STRINGER (John Wiley and Sons, New York).

[3] LICHTENBERG A. J. and LIEBERMAN M. A., *Regular and Stochastic Motion* (Springer-Verlag, New York, N.Y.) 1983.

[4] FEIGENBAUM M. J., KADANOFF L. P. and SHENKER S. J., *Physica D*, **5** (1982) 370; OSTLUND S., RAND D., SETHNA J. and SIGGIA E., *Physica D*, **8** (1983) 303.

[5] JENSEN M. H., BOHR T. and BAK P., *Phys. Rev. A*, **30** (1984) 960; OSTLUND S. and KIM S., *Phys. Scr.*, **T9** (1984) 193; CVITANOVIC P., SHRAIMAN B. and SODERBERG B., *Phys. Scr.*, **32** (1985) 263; KIM S. and OSTLUND S., *Physica D*, **39** (1989) 365; ECKE R., FARMER J. D. and UMBERGER D. K., *Nonlinearity*, **2** (1989) 175.